Optimal Cryogenic Processes for Nitrogen Rejection from Natural Gas

Homa Hamedi* [a], homa.h@u.nus.edu, Iftekhar A Karimi[a], cheiak@nus.edu.sg, Truls Gundersen[b], truls.gundersen@ntnu.no

a. Department of Chemical and Biomolecular Engineering, National University of Singapore.
Address: 4 Engineering Drive 4, Singapore 117585.
b. Department of Process and Energy Engineering, Norwegian University of Science and Technology.
Address: Kolbjorn Hejes v. 1A, NO-7491, Trondheim, Norway.

Abstract— Nitrogen rejection processes are usually needed for two natural gas sources: sub-quality natural gas reserves and produced gas from enhanced oil/gas recovery technologies. The nitrogen content of natural gas in the former is usually constant during the project lifetime, but it varies from 5 to 70% during enhanced oil/gas recovery programs. This variation leads to different process flowsheets for nitrogen removal: single-column, double-column, three-column, and two-column processes. In order to determine which configuration is more suitable for a particular nitrogen content in a feed stream, we must minimize the energy requirement for each process. In this study, we merge all the four configurations into two categories: single-column and multi-column processes and then use the Particle Swarm Optimization algorithm to optimize process parameters for each process with the objective of energy consumption minimization. Finally, we use the exergy concept to analyze theoretically these different processes.

Keywords— Cryogenic distillation, Cryogenic separation, Natural gas processing, Nitrogen-Methane separation, Nitrogen removal

1 Introduction

Natural gas (NG) is the cleanest and the most environmentally friendly fossil fuel with the highest hydrogen to carbon (H/C) ratio. Its combustion releases the most energy for the least CO2 emissions with minimal detrimental pollutants into the environment. Therefore, the utilization of low-quality NG (LQNG) reserves containing substantial amounts of non-hydrocarbon gases such as nitrogen, carbon dioxide, and hydrogen sulfide along with methane, has become attractive to gas processors. Of the aforementioned contaminants, nitrogen, diluting 57% of all LQNG reserves (Bradley Curtis III and Wess, 2008), can be considered as the most common impurity in NG resources worldwide. For instance, the Netherlands offshore region and North Germany in Europe, Mid-Continent and Rocky Mountain Foreland in the USA, and Kabir Kuh in Iran are some of the gas resources with high amounts of nitrogen (Krooss et al., 1995). The other major source of nitrogen contamination in NG is the Enhanced Oil and Gas Recovery (EOR/EGR) operations in which an inert gas such as nitrogen is injected into the reservoir and inevitably reproduced at the surface. The deployment of enhanced oil/gas recovery (EOR/EGR) is expected to expand progressively due to the depletion in reserve pressures worldwide (Höök, 2009). The "Thamama F" gas reservoir in Abu Dhabi is an example of nitrogen utilization for EGR (Borden, 2014). Examples of EOR processes are nitrogen flooding, leading to the production of nitrogen-rich associated gases, in the "Jay Oil Field", "Hawkins Field" and "Elk Hills" in the USA. A major difference between the nitrogen removal processes for EGR/EOR reservoirs and LQNG reserves is that the nitrogen content in the feed gas remains constant in the latter; while it may vary from 5-70 mole% in the former (MacKenzie et al., 2002).

Though not problematic in terms of toxicity or corrosion, nitrogen as a noncombustible gas that lowers the heating value of NG and makes NG out of the standard Wobbe index range and gas product requirements. Furthermore, the presence of nitrogen in the product gas increases costs due to the larger downstream equipment such as compressors and pipelines. Therefore, it is desirable to remove nitrogen and other contaminants from the LQNG/EOR/EGR sources. Among all the available methods for nitrogen removal such as cryogenic distillation, adsorption (N2-selective or CH4-selective), membranes, and hydrate-based gas separation, the first remains the leading technology for large-scale NG plants with capacities exceeding 0.5 million standard cubic meters per day

(MSCMD). The ability to reduce nitrogen to less than 1 mole% is another advantage of this method compared to the others (Rufford et al., 2012). However, cryogenic distillation is one of the most energy-intensive processes, as it may operate at as low as 93 K. This drawback has aroused interest in alternative methods for reducing cost and energy. In this context, a meaningful assessment of the various emerging methods demands a reliable work consumption benchmark for the incumbent cryogenic distillation.

Though several articles (Kuo et al., 2012; Rufford et al., 2012) compare the four above mentioned separation methods, only a limited literature examines the cryogenic processes in particular (Agrawal et al., 2003; Finn, 2013; GPSA, 2004). Mackenzie et al. (2002) in particular have very briefly compared the available basic cryogenic processes for a varying nitrogen content in the inlet NG feed (which will be elaborated in detail in the next sections). However, except some properties and conditions regarding the feed gas and product specifications, the authors do not provide any data on the process itself. For instance, compressor efficiencies and minimum temperature approaches, which greatly impact energy consumption in cryogenic plants, are not even given. More importantly, rather than comparing optimized processes, they just assume specific operating conditions for each process. Thus, their comparison is not strictly fair and accurate.

Four basic processes have been used for nitrogen rejection from natural gas: single-column, double-column, three-column, and two-column processes (Agrawal et al., 2003; Finn, 2013; GPSA, 2004; Healy et al., 1999; Kuo et al., 2012; Mackenzie et al., 2002; Rufford et al., 2012). The single-column process uses one cryogenic distillation column aided by one external refrigeration cycle. The absence of the external refrigeration cycle, which is used in LNG plants for feed gas with low nitrogen content, results in the waste of sales gas in produced nitrogen (Chen et al., 2016). The three other configurations, which are entitled the multi-column process in this study, operate based on the heat-coupled reboiler and condenser. The basis of the multi-column structure is the idea behind the double-column process, which was originally invented and widely used for ASUs to produce pure oxygen (Fu and Gundersen, 2012; Kerry, 2007). Section 2 is dedicated to the details of these processes.

The aim of this study is to compare the available cryogenic processes for nitrogen rejection from a natural gas feed in terms of their work requirements for varying nitrogen content in the feed. For this, each process is optimized separately using the particle swarm optimization method (Kennedy and Eberhart, 1995) to guarantee minimum work for given product and recovery/purity specifications. Thus, we present the process with minimum energy consumption for each nitrogen content in the feed. Finally, we use the concepts of exergy and the McCabe-Thiele diagram to explain why one process structure consumes less energy for the same separation than other alternative configurations.

2 Nitrogen Removal via Cryogenic Distillation

Though our study is applicable to both LQNG and EOR/EGR production programs, our main focus is the latter, where N2 can vary widely throughout the project lifetime. While the sales gas must be pressurized to enter the transmission network in both cases, the nitrogen product must also be recompressed in the latter for reinjection into the reservoir. A common specification (MacKenzie et al., 2002; Rufford et al., 2012) for pipeline transmission is 3 mole% max nitrogen in the sales gas. This spec can be achieved via cryogenic distillation, even though the feed NG may contain 5-70 mole% nitrogen. However, this wide variation in the N2 content poses a difficulty, as different process configurations may be required over the project lifetime. MacKenzie et al. (2002) describe several cryogenic distillation configurations such as single-column, double-column, three-column, and two-column.

2.1 Single-Column Design

Figure 1 illustrates the single-column process. It uses one cryogenic distillation column aided by one external refrigeration cycle in addition to Joule-Thomson expansions in two throttling valves (VL- 101 located on NG feed (SN-102) into the column and VL-102 on NG product (SN113) prior to the entry heat exchanger in Figure 1). We use a mixed refrigerant composed of methane and nitrogen as the working fluid. To maximize cold energy recovery, we merge all 2-stream heat exchangers into a multi-stream heat exchanger (MSHE-101). This heat integration gives us an opportunity to partly pre-cool the feed gas (SN-101) with the heating requirement of the boil-up stream (SN-111) which is wasted in a conventional process design. Also, one expander (E-101) is used in parallel with the sale gas product compressor (K-101). This modification decreases the energy consumption for feeds with lower nitrogen contents, where the pressure of SN-114 can be maintained to produce some work in the expander. Later, we will show via exergy analysis that for the lower-nitrogen feeds, the minimum reversible required work is negative. In other words, the input exergy is remarkably more than the process requirement. Each compressor in Figure 1 has three stages with interstage cooling using water. All three stages have the same pressure ratio for each compressor.

A key decision in this single-column design is the column pressure. Both column temperature and R (reflux ratio) decrease, as the pressure decreases. Although this lowers the refrigerant flow, it also decreases the minimum required temperature of the refrigerant (SN-117) which may lead to a higher work consumption in K-103. Similarly, lower column pressure also increases the power required for compressing the final product to its distribution pressure. Thus, a complex trade-off exits, and rigorous optimization is necessary. The other key operating parameters are the temperature of the column feed (SN-103 in Figure 1) and eight other key variables among which five control the refrigeration cycle operation.

Some literature (MacKenzie et al., 2002; Rufford et al., 2012) has reported that the single-column design fails to achieve a high methane recovery because the nitrogen-rich product even at near critical pressures cannot be liquefied and utilized as a reflux even if the refrigerant is at its minimum achievable temperature at near atmospheric pressure. However, note that even for a pure methane refrigerant and a pure nitrogen reflux, there exists a temperature difference of 10 K, which is much greater than the common minimum temperature approach of 2-3 K used for cryogenic processes.

2.2 Multi-Column Design

Figure 2 shows the multi-column process. It has a pre-fractionator, one high-pressure (HP) column, and one low-pressure (LP) column. In contrast to the single-column process, it needs no external refrigeration. The flowsheet in Figure 2 is a superstructure of various literature configurations such as the double-column, two-column, and three-column processes (Agrawal et al., 2003; Borden, 2014; Finn, 2013; Kuo et al. 2012; MacKenzie et al., 2002; Rufford et al., 2012). For instance, when the feed to the pre-fractionator is fully gaseous, then it becomes a double-column process, as the pre-fractionator can be eliminated. Similarly, when reflux flowrate for the HP-column (SN-216) is zero, the second column becomes a two-phase separator, and it becomes a two-column process. If these special cases are absent, then the process is a full three-column process.

All process streams are routed into a multi-stream heat exchanger in order to recover maximum cold energy. For an NG feed highly rich in nitrogen, additional nitrogen (SN-213) is taken out as a product from the HP column as done by Fu and Gundersen (2012), and Kerry (2007) for air separation units (ASU). Similar to the single-column design, one parallel expander is considered for K-201 and each compressor in Figure 2 has three stages with water intercoolers.

It is notable that the pivot of the multi-column structure is the idea behind the double-column process, which was originally invented for ASUs to produce pure oxygen (Fu and Gundersen, 2012; Kerry, 2007). Here, the separation occurs in two columns (instead of one column) at different pressures to provide the cooling of the reflux in the HP column using the bottom product of the LP column. This energy exchange happens in a condenser-reboiler heat exchanger (HE-201). To meet the minimum temperature approach for this heat exchange, the LP column pressure must be lowered as necessary. The difference between the HP and LP column pressures is directly proportional to the difference in the normal boiling point temperatures of the top and bottom products. For instance, this difference is 12.8 K for oxygen and nitrogen, but 34.3 K for nitrogen and methane. Thus, the HP column needs a considerably higher pressure than the LP column for the latter. Thus, while the double-column process is an attractive and common design for ASUs with 500 to 600 kPa pressure difference between the two columns (Fu and Gundersen, 2012; Kerry, 2007); the same configuration for nitrogen and methane might not be as attractive due to a much higher pressure drop of more than 2000 kPa for a highly nitrogen-rich feed. The higher pressure drop increases the recompression costs.

The multi-column process involves more complex decisions and trade-offs in contrast to the single-column process, hence rigorous optimization is again warranted.

2.3 Process Design Data

The specifications that form a common basis for comparing the single-column and multi-column designs are listed in Table 1. Feed conditions, which are the downstream conditions of a turbo-expander-based natural gas liquids recovery unit, were assumed based on the data from Mackenzie et al. (2002). They assumed a 2-component feed (methane and nitrogen), which is reasonable after the turbo-expander unit, and we did the same for a fair comparison. We assumed all reflux streams to be saturated liquids, and all boil-up streams to be saturated vapors. We assumed 15 equilibrium stages for both the rectifying and stripping sections. This is sufficiently larger than what is required for the range of separations in this study. Excess stages are assumed to minimize the reflux ratio and in turn, the refrigeration requirement (McCabe and Thiele, 1925; Timmerhaus and Flynn, 1989). We ensured this by checking the composition graph (see a sample in Appendix A) for each column. The presence of dummy stages near the feed stage suggests excess stages.

Table 1. Design data and specifications

Design Specification	Value
Feed Flowrate, MSCMD	28.32
Feed Pressure, kPa	6000
Feed Temperature, °C	25
Compressor and Expander Adiabatic Efficiency	0.75
Min Temperature Approach in MSHEs, °C	2
Pressure Drop for MSHE, kPa	20
Min Temperature Approach in Condensers/Reboilers, °C	2
Minimum Methane Recovery, mole %	98
Maximum Nitrogen Impurity in Product, mole %	3
Nitrogen Product Pressure, kPa	3447
NG Sales Gas Pressure, kPa	1827
Pressure Drop for each Rectifying Section, kPa	10
Pressure Drop for each Stripping Section, kPa	10
Number of Stages for each Rectifying Section	15
Number of Stages for each Stripping Section	15
Tray Efficiency, Percentage	100

Cooling Water Temperature, °C	293.15
Min Temperature Approach for Cooling Water Heat Exchanger, °C	5

3 Parametric Optimization

Heuristic methods such as Particle Swarm Optimization (PSO), Simulated Annealing (SA) and Genetic Algorithm (GA) have been shown to be effective on problems that are not solved well by conventional optimization. Unlike non-linear programming and local search methods, the heuristic approaches with an interaction between local improvement procedures and higher level strategies create a robust global optimization search of a solution space which is probably multimodal. These approaches are also categorized as non-derivative optimization methods because they do not take advantage of any information about the problem structure. Consequently, they can tackle complex nonlinear models and are suitable for problems with objective functions evaluated by black-box software. All the characteristics stated for heuristic methods are applicable for the problem under investigation.

The stochastic PSO technique is widely used for continuous optimization. This method has been successfully applied for rigorous optimization in many chemical engineering areas in past several years (Cao et al. 2017; Clarke et al., 2014; Khan and Lee, 2013; Rezakazemi et al., 2017; Sadeghzadeh et al., 2015; Siddhartha et al., 2012). It is demonstrated that PSO gets better results in a faster, cheaper way compared with other heuristic methods (Eghbal et al., 2011; Elbeltagia et al., 2005; Hassan et al. 2005; Panduro and Brizuela, 2009). Another reason that PSO is preferred over other methods is that there are few parameters to be specified by users (Khan and Lee, 2013). Unlike the genetic algorithm approach, , which seems the most popular evolutionary optimization method, PSO was originally invented for continuous searching and does not need any coding and decoding for this type of problems. Thus, it reduces running time. The aforementioned advantages become an incentive to choose this method for the current rigorous optimization.

In this section, the operating parameters (or decision variables) and constraints are presented for each design, which are optimized using the Particle Swarm Optimization method (PSO) (Kennedy and Eberhart, 1995) to find the minimum energy requirements for various N2-contents in the NG feed.

The PSO method was programmed in Matlab with relative convergence of each variable as the termination condition or no changes in fitness function values after 30 consecutive iterations. Table 2 presents the PSO parameter values used in this study (please refer to Kennedy and Eberhart (1995) for the parameters ‘interpretation). The algorithm was linked with Aspen Hysys V.9, which was used to simulate each random design generated by the PSO. The Soave Redlich Kwong (SRK) property method was used in Aspen Hysys. “Modified HYSIM inside-out” was selected as the default column simulation algorithm. Two other methods, namely HYSIM inside-out and sparse continuation, were also used if a column did not converge.

Table 2. PSO parameters used for optimization in this study

PSO Parameters	Value
Min inertia weight	0.5
Max inertia weight	1
Global acceleration factor	1
Personal Acceleration Factor	1
Particle size for each variable	40

Since the PSO generates random inputs during optimization, an input may not necessarily give a feasible process, and Aspen Hysys simulation may not converge. In such cases, the energy consumption was set to be a large value. Warning messages generated by Aspen Hysys in these instances interrupt optimization. This was resolved by activating the "Display errors in trace window" option in Aspen Hysys. This activation sends all the messages to the trace window instead of popping up on the flowsheet view and interrupting the program.

3.1 Single-Column Process Optimization

For the single-column process, the main energy consumers are the three 3-stage compressors, K-101, K-102, and K-103. One expander (E-101) may produce some of the energy needed by them. Hence, the objective for the optimization problem is to minimize the net total energy consumption.

$$\text{Objective Function} \quad \text{Total Work Consumption} = W_{K-101} + W_{K-102} + W_{K-103} - W_{E-101} \qquad \text{Eq. 1}$$

Where W represents the required or produced work by the corresponding subscripted compressor or expander.

Table 3 lists the 10 operating parameters selected as the decision variables for this optimization. The streams and equipment are as labeled in Figure 1.

Table 3. Decision variables for the single-column process

Name	Operating Parameter	Module	Stream / Equipment
x1	Pressure	SN-103	Feed to T-101
x2	Temperature	SN-103	Feed to T-101
x3	Pressure	SN-119	Refrigerant stream from K-103
x4	Molar Flow Rate	SN-119	Refrigerant
x5	Nitrogen Mole Fraction	SN-119	Refrigerant
x6	Temperature	SN-121	Refrigerant to VL-103
x7	Pressure Drop Ratio	VL-103	Valve on SN-121
x8	Pressure Drop Ratio	VL-102	Valve on sales gas stream (SN-113)
x9	Temperature	SN-108	Nitrogen product
x10	Temperature	SN-115	Sales gas product

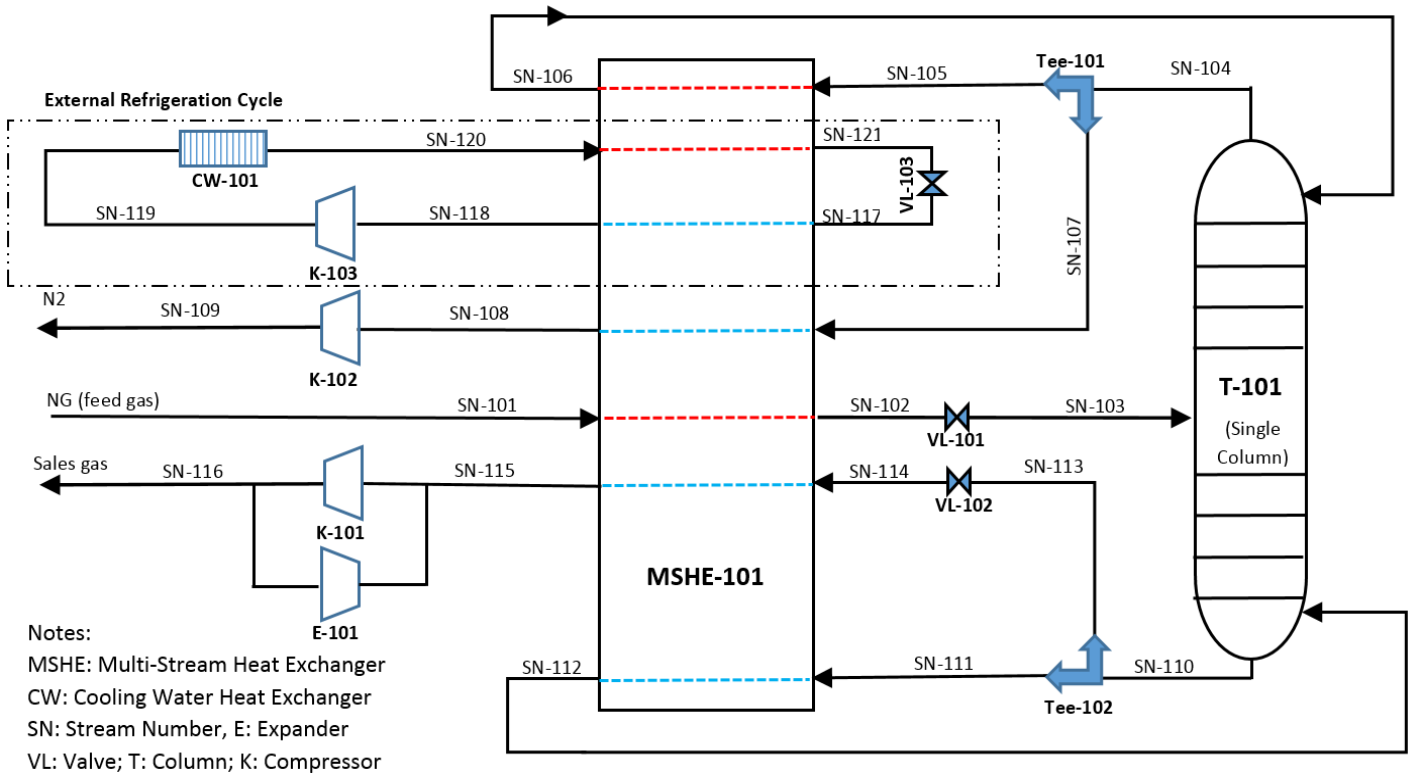

Figure 1. Single-column process flow diagram (Rufford et al. 2012)

The following specs must be achieved for this process, which are the constraints:

$$Methane\ Recovery \geq 98\% \quad \text{Eq. 2}$$

$$Nitrogen\ mole\%\ in\ Sales\ Gas \leq 3\% \quad \text{Eq. 3}$$

$$Minimum\ Temperature\ Approach\ in\ (MSHE - 101) \geq 2K \quad \text{Eq. 4}$$

It is obvious that the work will be the minimum, when the first two constraints (Eq. 1 and Eq. 2) are active. This allowed us to use a distillation column sub-flowsheet with methane recovery and nitrogen impurity as specs instead of an absorber column sub-flowsheet in Aspen Hysys to simulate T-101 in Figure 1. The conditions of the reflux and boil-up streams from inside the distillation column sub-flowsheet were copied to the corresponding streams involved in MSHE-101. This trick eliminated the first two constraints, and Eq. 3 was added as a penalty term to the objective function.

At some pressures and temperatures, the liquid phase of SN-103 may have <3 mole% nitrogen. In this case, the column cannot converge for the nitrogen impurity spec of 3 mole%. It is obvious that this cannot be an optimal solution, because stripping the bottom product to a higher purity should require more work. Therefore, the minimum value of 3 mole% for nitrogen mole fraction in the liquid phase of SN-103 is chosen as a column spec.

3.2 Multi-Column Process Optimization

The multi-column design (Figure 2) has four product compressors (K-201, K-202, K-203 and K-204), one expander (E-201) in parallel with K-201, and one pump (P-201), hence the objective again is to minimize the net total power consumption. The

optimization involves the 15 decision variables process listed in Table 4 and shown in Figure 2. The following constraints were added as penalty terms to the objective function for this process:

$$Methane\ Recovery \geq 98\% \quad \text{Eq. 5}$$

$$Nitrogen\ mole\%\ in\ Sales\ Gas \leq 3\% \quad \text{Eq. 6}$$

$$Minimum\ Temperature\ Approach\ in\ MSHE - 201 \geq 2K \quad \text{Eq. 7}$$

$$Minimum\ Temperature\ Approach\ in\ HE - 201 \geq 2K \quad \text{Eq. 8}$$

T-201 in Figure 2 was simulated using a reboiled absorber column sub-flowsheet instead of an absorber column sub-flowsheet. The desired nitrogen impurity in SN-206 was used as a column spec, which eliminated the split ratio for SN-206 in Tee-201 as an optimization variable.

If and when SN-203 is completely vapor, the pre-fractionator T-201 is eliminated (equivalent to the double column design), SN-201 passes MSHE-201 twice with one throttling valve (VL-201) in the middle. In both instances, it acts as a hot stream in MSHE-201. Reducing its temperature through VL-201 is not desirable for heat integration, hence the pressure drop through VL-201 is set to zero, when SN-203 is completely vapor.

Table 4. Decision variables for the multi-column design.

Name	Operating Parameter	Module	Stream / Equipment
x1	Pressure	SN-203	Feed to T-201
x2	Temperature	SN-203	Feed to T-201
x3	Nitrogen mole fraction	T-201	SN-206 and spec for T-201
x4	Pressure Drop Ratio	VL-202	Valve on Sales Gas Stream (SN-206)
x5	Pressure	SN-211	Feed to T-202
x6	Vapor Fraction	SN-211	Feed to T-202
x7	Pressure	SN-222	Feed to T-203
x8	Vapor Fraction	SN-222	Feed to T-203
x9	Split Flowrate Fraction	Tee-203	Reflux to T-203 (SN-217)
x10	Split Flowrate Fraction	Tee-202	Excess nitrogen to K-204 (SN-213)
x11	Vapor Fraction	SN-220	Reflux stream to T-203
x12	Pressure	SN-227	Sales gas from P-201
x13	Temperature	SN-229	Sales gas from pre-fractionator
x14	Temperature	SN-231	N2-rich product from T-203
x15	Temperature	SN-232	N2-rich product from T-202

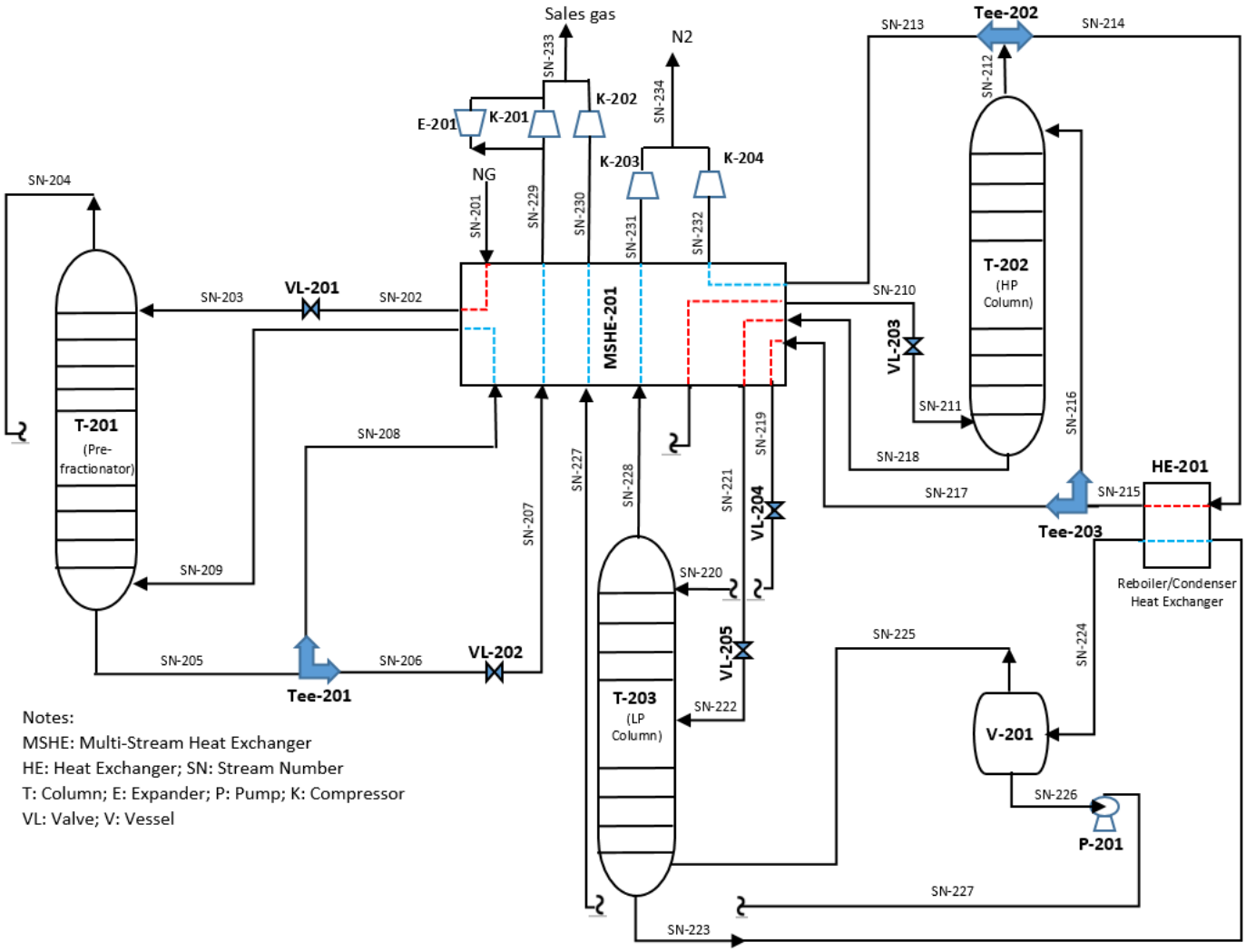

Figure 2. Process flow diagram for the multi-column design.

4 Results

The two process designs for each nitrogen content were optimized using the PSO program. Each PSO algorithm trial converged after almost 20 hours for the single-column design and 65 hours for the multi-column design. The number of trials was set at three. There is a very insignificant difference among the three optimal solutions, which implies that the algorithm is most probably converging to the global optimum. Nevertheless, any stochastic method cannot guarantee the convergence to the global optimum. However, the best of the three objective function values was still taken as the optimal. All computations were done on an Intel® Core (TM) i5-6600 workstation with 3.3 GHz CPU and 16 GB RAM. The optimal values for the decision variables for the two designs are provided in Tables 5 and 6 respectively.

As Table 5 shows, the single-column inlet pressure (*x1*) decreases as the feed nitrogen increases from 5% to 50%; however, this trend reverses as the nitrogen goes beyond 50%. It is logical that the column operating pressure is reduced to decrease the reflux flow for higher nitrogen contents in the feed. This reduces the refrigerant flow and hence the compression work associated with it. Nonetheless, one should note that the ultimate pressure of the nitrogen-rich product (3447 kPa) is 1.89 times the sale gas pressure

(1827 kPa). This could also explain why the system operates at higher pressures for nitrogen contents above 50%. The same trend is observed for the column feed temperature (*x2*). For 30%-50% nitrogen content, with the lowest column pressures or correspondingly the lowest reflux temperatures, the pressure ratio of VL-103 (*x7*) reaches zero, equivalent to 121.325 kPa (atmospheric pressure plus MSHE pressure drop) for SN-117. This stream has the coldest temperature in the system and is responsible for providing the cooling requirement of the reflux stream. In addition, only for 5% nitrogen, the process employs the sales gas outlet expander.

Table 6 suggests that the switch from the three-column to the double-column structure occurs between 40% and 50% nitrogen. For 5-10% nitrogen, the optimal pre-fractionator pressure shows a gradual decrease from 2788 to 2594 kPa, which is followed by a remarkable decline to 2148 kPa for 20% nitrogen. This behavior can be explained by the fact that for the former cases, the system utilizes the sales gas outlet expander and prefers to keep the column pressure high; however, for 20% nitrogen, a pressure drop after the throttling valve (VL-201) plays a more important role since it produces a larger amount of liquid slug to get processed in the pre-fractionator. As the inlet nitrogen increases beyond 40 mole%, the pre-fractionator becomes less significant and disappears at 50% nitrogen. Thus, the process shifts to the double-column design. The vapor fraction of the inlet stream into the pre-fractionator, shown inside the parentheses, increases as nitrogen content increases. In order to minimize the minimum temperature approach in HE-201 (Figure 2), the HP column pressure, represented by *x5* in the table, also increases with the inlet nitrogen percentage.

Figure 3 shows the minimum energy consumption per unit feed (kW/MSCMD) for the two process designs over the range of 5-70% nitrogen content in the NG feed. As depicted in Figure 3, the single-column design consumes more energy than the multi-column design for nitrogen contents below 50-60%. As the nitrogen content increases, the energy consumption also increases for both designs. However, the rise is slower for higher nitrogen contents. For 5% nitrogen, the single-column design needs 83.60 kW per MSCMD of NG feed (189.0 kW total consumption by the compressors and 105.4 kW production by the expander). This value increases to 1990 kW/MSCMD for 70% nitrogen. For the multi-column design, the energy consumption spans from -39.58 to 2170 kW/MSCMD for 5 and 70 mole % nitrogen respectively. In other words, at 5% nitrogen, most of the sale gas is produced in the pre-fractionator (T-201) which operates at the pressure (2788 kPa) significantly higher than the product pressure (1827 kPa). Thus, thanks to the expander E-201 and low refrigeration requirement in MSHE-201, this design can generate 39.58 kW/MSCMD net work at 5% nitrogen. For the multi-column design, the consumption curve changes slope between 40% and 50% nitrogen. This occurs due to the change from a three-column design to a double-column design. In other words, the three-column design is the best for less than 40-50% nitrogen in terms of energy consumption. Clearly, the pre-fractionator plays a key role in reducing energy consumption for 5% to 40% nitrogen. It extracts a large portion of the inlet methane at high pressure. Finally, the two-column design can be used for nitrogen percentages less than 20% since SN-216 flowrate is negligible for these cases and T-202 can be replaced by a two-phase separator.

Figure 3 also shows the reduction (%) in energy consumption for the multi-column versus single-column design. As can be observed, the relative energy saving is higher for lower nitrogen contents and decreases gradually until it reaches zero at 55 mole% and negative values for higher nitrogen contents. Given a larger number of equipment and higher associated maintenance cost, as well as higher complexity in the multi-column system compared to the single-column process, this configuration might be considered only for lower nitrogen contaminations where high reduction rates in energy consumption are achievable. Nonetheless, further economic analysis is required prior to deciding the optimum process design based on the governing energy regulations and circumstances, which is out of the scope of this study.

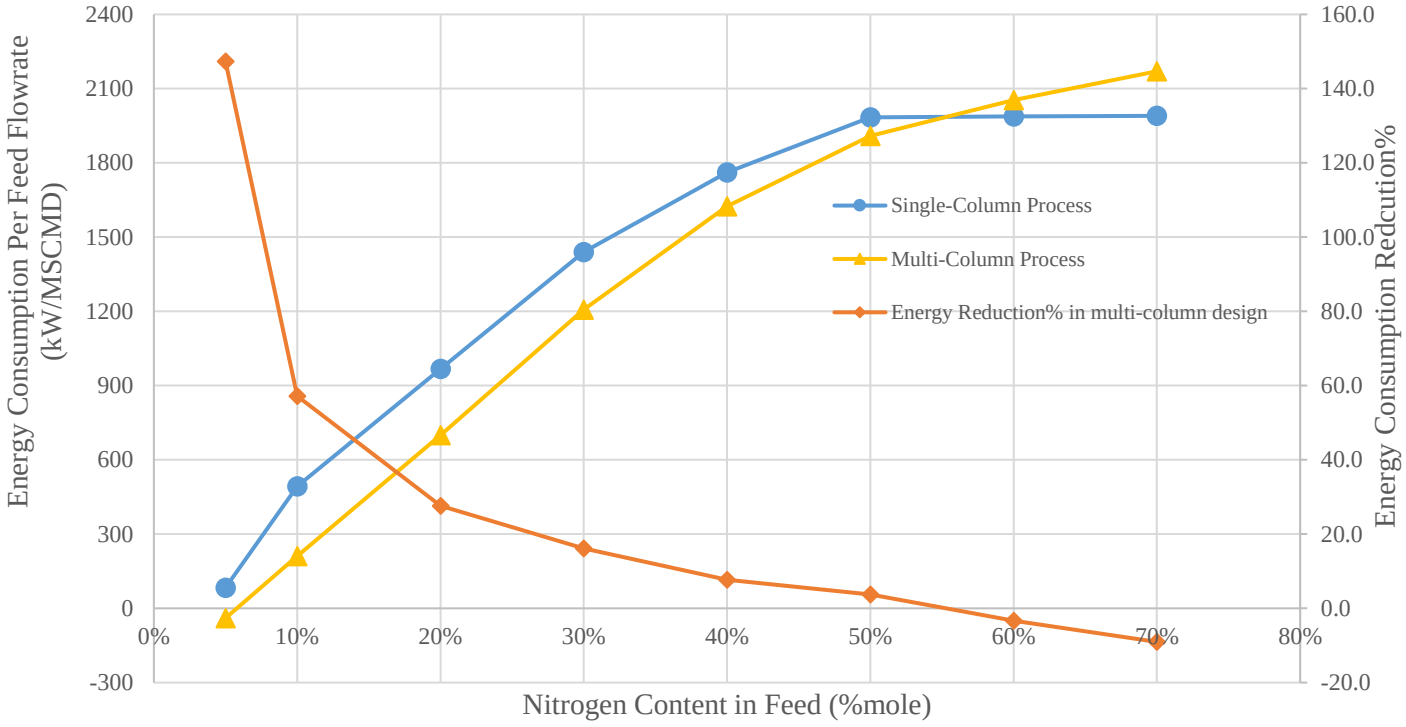

Figure 3. Work consumption for nitrogen removal processes: single-column design and multi-column design. Multi-column design corresponds to the three-column process for nitrogen ≤ 40 mole% and the double-column process for nitrogen ≥ 50 mole%)

Figure 3 shows that with respect to increasing nitrogen content in the feed, the energy consumption of the both processes monotonically increases with a decreasing rate. However, the energy consumption of the single-column process remains almost constant while nitrogen content increases from 50 to 70%. To explain these behaviors, the theoretical minimum work requirement to perform the separation reversibly is presented in Figure 4. This value is negative for lower nitrogen cases, 5 mole% to 33 mole%, which means that work can be achievable if the process takes place reversibly and increases to positive values as nitrogen contamination increases in the inlet gas. According to this figure, the theoretical minimum work levels out around 70 mole% nitrogen and then declines. One may expect the maximum occurs at 50 mole% as the mixing entropy production (or equivalently minimum required work for separation) of a binary regular mixture, which can be calculated by Eq. 11, is highest when the ratio is 50:50.

$$Produced\ Entropy_{mixing} = -nR\ (x\ Lnx + (1-x)\ Ln(1-x)) \qquad Eq.\ 11$$

Where n, R and x are the total number of moles, gas constant and mole fraction (Kotas, 1995).

However, the pressure of nitrogen product (3447 kPa) is much higher than that of sales gas product (1827 kPa). Therefore, having higher nitrogen in the feed leads to higher net compression work. Thus, due to the contrary effects of the two mentioned facts, the theoretical minimum required work experiences a stabilization followed by a decreasing rate as the nitrogen content increases. This can verify the trends in Figure 3 in which the real work consumption increases at a decreasing rate for both single-column and multi-column designs. However, in the single-column process, the value stabilizes at 50 mole% nitrogen compared to 70% in the

theoretical minimum required work graph. This hastened stabilization in the single column as a real process is because of the higher irreversibility rate (which will be shown in Figure 5) in all main equipment at 50% compared to 60% and 70%.

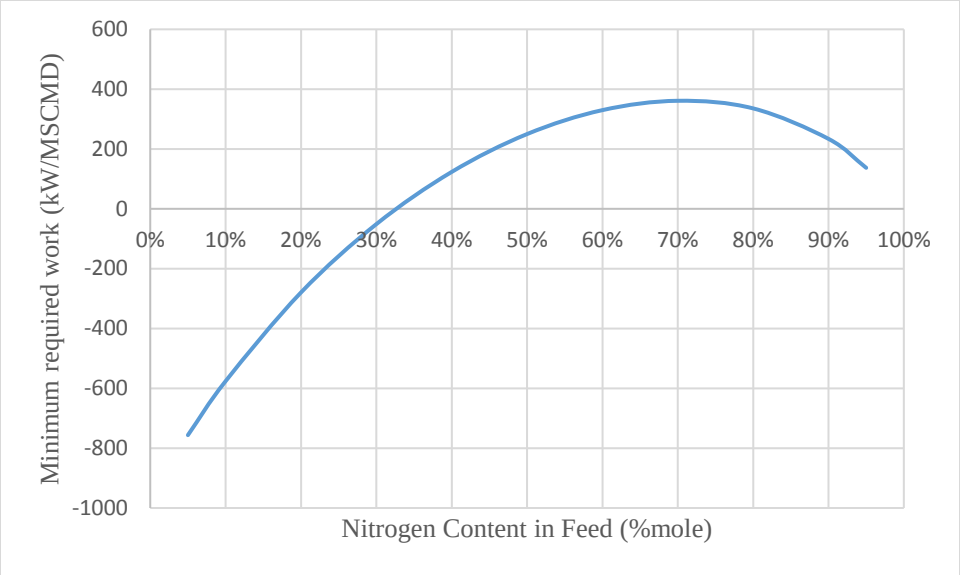

Figure 4. Theoretical minimum required work for 5-95% nitrogen in the inlet gas

Table 5. Optimal operating parameter values for the single-column design

N2 mole% / Decision Variables [1]	5%	10%	20%	30%	40%	50%	60%	70%
x1 (kPa)	2849	2654	2247	2039	1864	1813	2692	2676
x2 (K)	167.0	162.0	150.6	141.7	273.4	273.5	273.7	273.8
x3 (kPa)	2194	1849	1477	2106	1967	2081	2858	2820
x4 (kmole/s)	0.05	0.09	0.10	0.09	0.11	0.11	0.16	0.15
x5	0.00	0.00	0.00	0.00	0.02	0.04	0.03	0.02
x6 (K)	148.2	126.6	119.6	118.9	116.9	113.2	118.5	118.9
x7 $(kPa)^2$	487.5	259	161.3	121.3	121.3	121.3	205.4	198.0
x8 $(kPa)^2$	2200	1830	1447	1136	995.5	853.7	838.9	683.8
x9 (K)	220.4	223.6	226.6	234.1	253.9	262.4	257.5	250.9
x10 (K)	229.7	236.4	239.6	238.8	231.7	222.2	240.9	245.8

1. Variables are mentioned based on Figure 1 and Table 3
2. For the convenience of readers, the corresponding downstream pressure of the valve is presented instead of its pressure drop ratio

Table 6. Optimal operating parameter values for the multi-column design

N2 mole% / Decision Variables[1]	Three-Column Structure					Double-Column Structure		
	5%	10%	20%	30%	40%	50%	60%	70%
x1 (kPa) [2]	2788 (0.00)	2594 (0.03)	2148 (0.17)	2842 (0.66)	3083 (0.81)	3083 (1)	3083 (1)	3083 (1)
x2 (K)	168.4	162.2	150.8	160.0	158.6	156.0	150.8	144.9
x3	0.0269	0.0198	0.0087	0.0188	0.0141	NA	NA	NA
x4 (kPa)[3]	2360	2040	1542	1840	1602	NA	NA	NA
x5 (kPa)[3]	1925	1988	1990	1993	2292	2374	2397	2722
x6	0.0933	0.1974	0.3549	0.2694	0.3246	0.3898	0.4944	0.6097
x7 (kPa)	386.0	458.0	470.1	343.0	384.2	298.1	262.1	287.7
x8	0.1350	0.1362	0.1580	0.2003	0.2063	0.2320	0.2482	0.2683
x9	0.07	0.44	0.39	0.54	0.55	0.28	0.16	0.66
x10	0.48	0.29	0.43	0.20	0.11	0.26	0.36	0.12
x11	0.3420	0.2542	0.2257	0.0514	0.3325	0.1325	0.0482	0.2226
x12 (kPa)	1827	1435	861.7	1119	1088	NA	NA	NA
x13 (K)	221.7	221.6	221.7	221.1	191.8	NA	NA	NA
x14 (K)	123.2	153.8	161.5	181.3	203.4	190.3	199.6	221.3
x15 (K)	193.5	181.2	156.3	195.4	206.3	221.6	213.0	221.0

1. Variables are mentioned based on Figure 2 and Table 4
2. Values in parentheses are the corresponding vapor fraction of SN-203; vapor fraction equal to one means the double-column design
3. For the convenience of readers, the corresponding downstream pressure of the valve is presented instead of its pressure drop ratio
4. NA: Not Applicable (not applicable for the double-column process)

5 Exergy Analysis

Exergy is defined as the maximum amount of work that can be produced by a stream or system as it is brought into equilibrium with a reference environment, and it can be thought of as a measure of the usefulness or quality of energy. Energy and exergy balances can be written for a general process or system. However Energy is subjected to the conservation law, whereas exergy, a measure of energy quality or work potential, can be consumed due to irreversibilities in real processes (which is proportional to entropy production) and conserved during ideal processes. Compared to energy analysis, exergy analysis gives a better thermodynamic measure of process efficiency. In simpler words, the higher exergy losses, the less efficient an operation unit is. For a detailed procedure of exergy calculations, please refer to Hinderink et al. (1996) and Kotas (1995).

The exergy analysis can explain the difference in energy consumptions of the two designs (single-column and multi-column), as illustrated in Figure 3. Figure 5 shows the distribution of the exergy losses among various equipment in the two designs. According to this figure, the multi-column design improves process efficiency by reducing substantially exergy losses in distillation columns for all nitrogen contents. This advantage can be observed also for heat exchangers, compressors, pumps and the expander when nitrogen content is less than 50-60 mole%. The differences decrease with nitrogen contents until they become almost equal to zero at some point between 50-60 mole%. Though for higher nitrogen percentages, the total exergy degradation rate in columns is still

lower compared to the single column design, the multi-column design loses a larger amount of exergy in other equipment. This results in a higher energy consumption for the latter. Furthermore, the pressure-based exergy depletion rate through the Joule-Thomson valves in the multi-column design is larger than the single-column design. This trend can be expected because a high-pressure drop occurs between the HP column and the LP column. Finally, the "others" category in Figure 5 refers to exergy degradation in mixers and cooling water systems, and external exergy losses from the material and waste heat streams entering the environment.

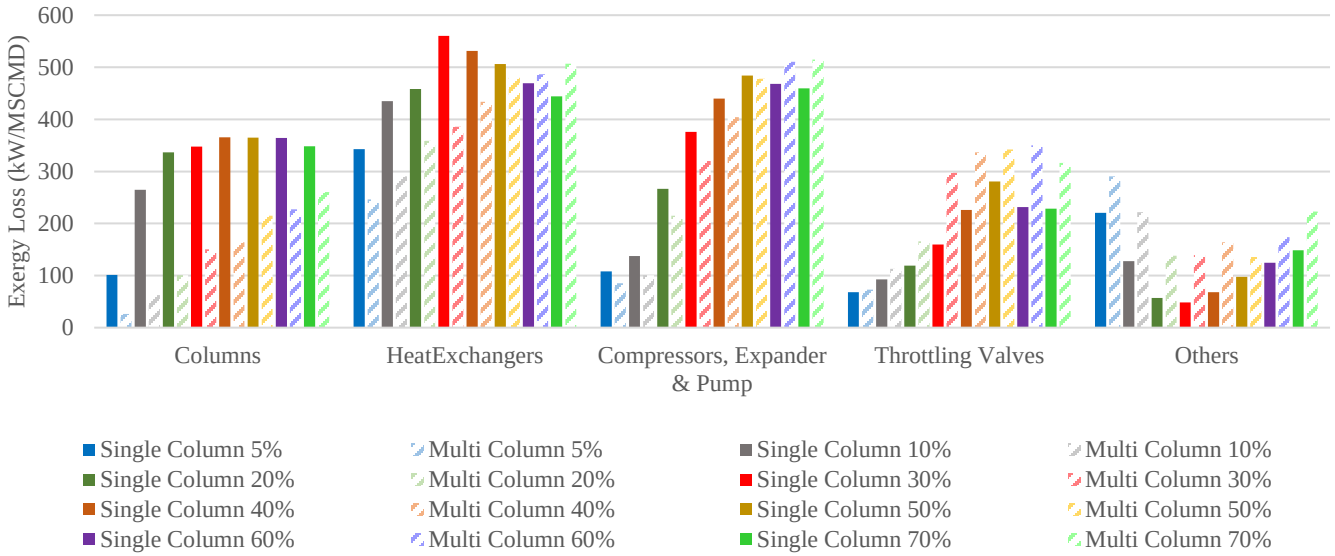

Figure 5. Exergy loss distribution for 5-70% nitrogen in the inlet gas

The final discussion of this paper is dedicated to explaining why the exergy degradation in columns is always lower in the multi-column process. For this purpose, consider an NG feed with 50% nitrogen, which uses the double-column structure because the vapor fraction of the pre-fractionator feed is one.

It can be reasonably assumed that the output temperatures gradually come to the ambient condition (298.15 K) as they flow through the outlet pipeline and consequently, their temperature-based exergy values are negligible. With this assumption, the theoretically minimum required work based on the exergy loss from the input to the output material streams is estimated as 249.82 kW/MSCMD. In other words, if this separation is performed reversibly, then only 249.8 kW/MSCMD of work would be required. Nevertheless, according to Figure 3, the separation actually needs 1983.7 and 1909 kW/MSCMD for the single-column and double-column designs respectively. Therefore, irreversibility values can be calculated as 1733.9 and 1659.2 kW/MSCMD, and the exergy destruction in distillation columns (see Figure 5) are 365.1 and 214.7 kW/MSCMD respectively. As a result, 21% and 13% of the total irreversibilities in single-column and double-column designs correspond to the distillation columns respectively.

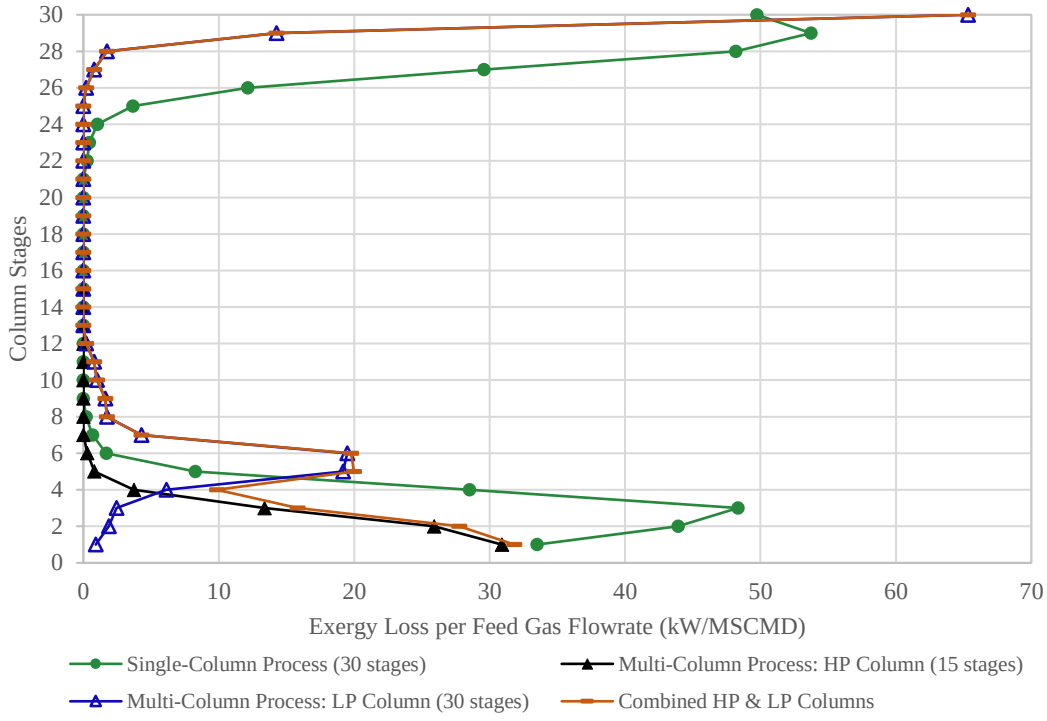

Figure 6. Exergy loss profile in columns (stages numbered from top to bottom)

The exergy degradation in distillation columns occurs due to finite driving forces, mixing, and pressure drop. If the separation is done reversibly, then the operating lines coincides with the equilibrium curve and the exergy loss is zero. However, the reversible separation is not possible in practice since it requires a column with infinite stages and infinitely many side exchangers. In reality, distillation columns lose exergy due to various irreversibility which is directly proportional to the distance between the operating lines and the equilibrium curve. In other words, as the operating line becomes far from equilibrium line, which means higher entropy production due to larger finite driving forces, the exergy loss (the lost work) becomes larger and the required work for the separation increases (Soares Pinto et al., 2011). Figure 6 compares exergy dissipation in columns for the two designs. The total exergy destruction in the single-column design is larger than that in the double-column design. This difference can be explained by the McCabe-Thiele diagram (McCabe and Thiele, 1925) in Figure 7.

Figure 7 reveals how a double-column design reduces irreversibility. As seen in Figure 7a, the single-column design has irreversibilities in both the stripping and rectifying sections. On the other hand, if the separation is conducted in two steps as in a double-column design (Figure 7b), the exergy dissipation is not significant in the HP column and moderate in the LP column. One should note that the reboiler stage (appearing as a separator in Figure 2 and a triangle at the lower part of the blue diagram in Figure 7) should be excluded in the LP column diagram. The following question may be raised: Even though the area between the operating and equilibrium lines in the LP column seems to be larger than for the single-column design, Figure 6 shows lower exergy loss in the LP column compared to the single column. This result can be explained by the fact that some nitrogen is extracted from the HP column top and so the feed rate into the LP column is lower (a 25% reduction for the case of 50% nitrogen). This reduction in feed flowrate gives a lower exergy loss in the LP column. It should be noted that according to Figure 6, there are no exergy losses in the middle trays. This is because the number of stages was assumed large enough for the separation process to minimize the reflux rate,

and consequently the operating costs. Thus, the middle trays are actually dummy trays, where the equilibrium and operating lines are very close and driving forces are close to zero.

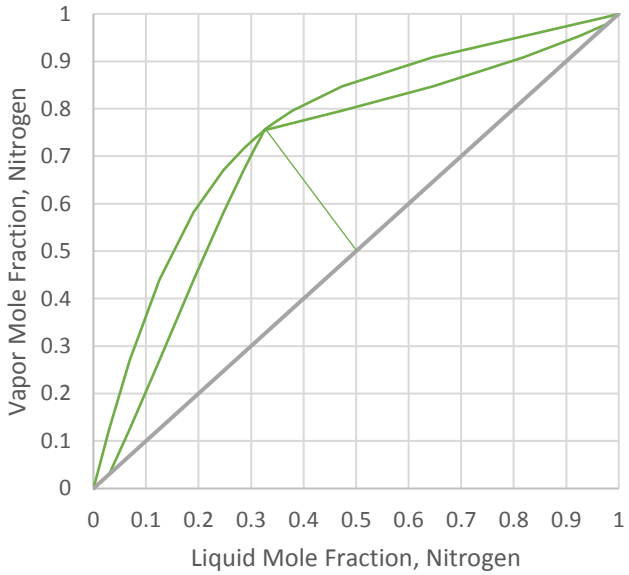

Figure 7a. McCabe-Thiele diagram for the single-column separation (inlet column pressure: 1813 kPa)

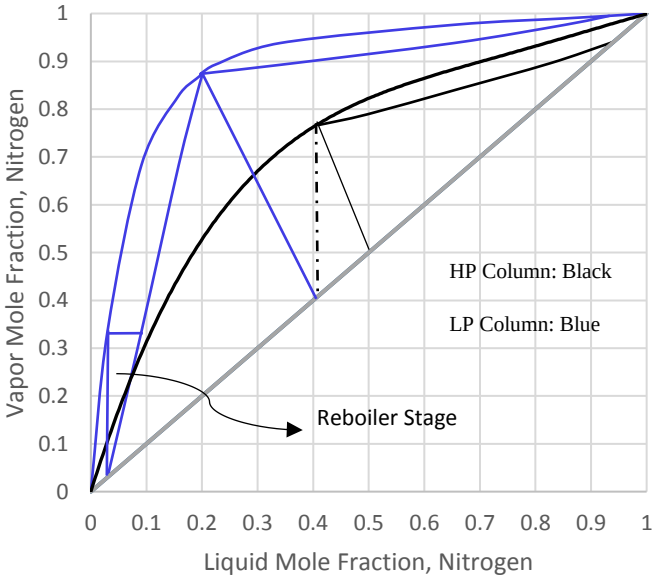

Figure 7b. McCabe-Thiele diagram for the multi-column separation (HP-column pressure: 2374 kPa, LP-column pressure: 298.1 kPa)

6 Conclusions

Nitrogen removal from natural gas is important in LQNG production and EOR/EGR programs. The main difference between the two processes is nitrogen content variation in the inlet gas through EOR/EGR programs. These changes in nitrogen contamination lead to different process designs, each of which is suitable for a particular range of nitrogen content. In order to be able to compare the processes, we need to minimize energy consumption of each process. For this purpose, we proposed two configurations: single-column design and multi-column design. The latter includes three common processes in the literature for nitrogen rejection: double-column, three-column and two-column structures. The model can be simulated by the Aspen HYSYS flowsheet simulator and optimized using the stochastic PSO technique programmed in MATLAB. This investigation proves that a single-column process needs more energy to perform the separation compared to other configurations for feed nitrogen contents less than 55 mole% and less energy for higher nitrogen content. Also, the two-column process is almost equivalent to the multi-column process for lower nitrogen contents (<20%). The multi-column process can reduce exergy degradation in columns for all nitrogen contents and when the values are less than 50%, a decreasing trend can be observed for heat exchangers and compressors. These reductions in exergy destruction rate can be investigated using exergy analysis, column exergy loss profiles and McCabe-Thiele diagrams.

However, this study reveals that the energy consumption difference between multi-column and single-column process is not as significant as previous work has presented without any process optimization (MacKenzie et al., 2002). In addition, due to a larger quantity of equipment and higher associated maintenance cost, as well as higher complexity in the multi-column system compared to the single-column process, this configuration might not be an attractive configuration for nitrogen rejection in EOR/EGR programs. Nonetheless, a further economic analysis is required prior to deciding the optimum process design based on the governing energy regulations and circumstances, which is out of the scope of this study.

Appendix A

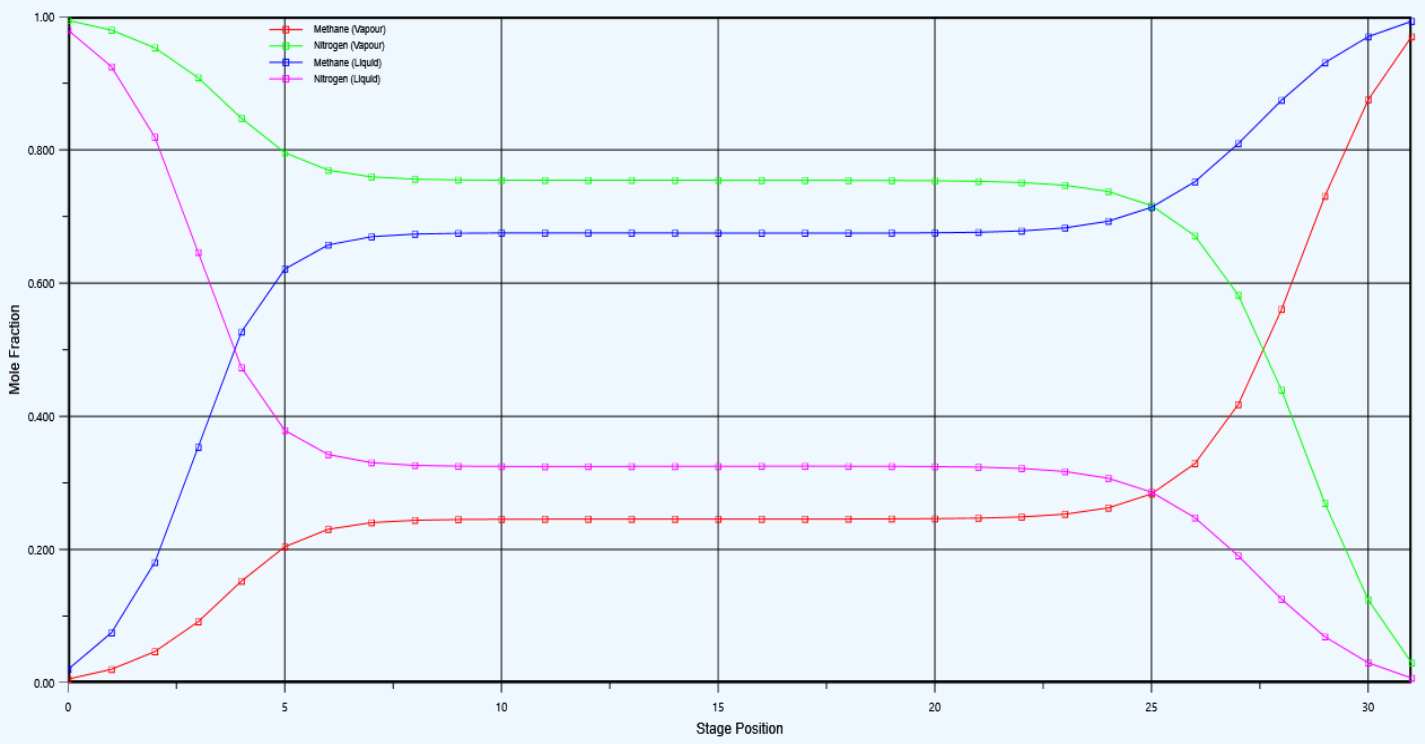

Figure A.1. Composition versus column stages in a single-column process for 50 mole % nitrogen in the feed gas

7 References

Agrawal, R., Herron, D.M., Rowles, H.C., Kinard, G.E., 2003. Cryogenic Technology, Kirk-Othmer Encyclopedia of Chemical Technology, 8. John Wiley & Sons.

Borden, K., 2014. Enhancing megaprojects through innovation, IPTCDAILY, The official show daily of the international petroleum technology conference, Qatar.

Bradley Curtis III, A., Wess, M., 2008. Commercialization of nitrogen-rich natural gas, School of chemical, biological and material engineering, The University of Oklahoma, http://www.ou.edu/class/che-design/a-design/projects-2008/LQNG.pdf

Cao, Y., Flores-Cerrillo, J., Swartz, C.L.E., 2017. Practical optimization for cost reduction of a liquefier in an industrial air separation plant, Computers and Chemical Engineering, 99, pp. 13-20.

Chen, F., Okasinski, M., Sabram, T., 2016. Novel Nitrogen Removal Schemes for LNG Plants with Electric Motor Drive and Varying Feed Composition, Air Products and Chemicals, Inc., http://www.airproducts.com/~/media/Files/PDF/company/company-overview/news-center/LNG18-nitrogen-removal.pdf

Clarke, J., McLay, L., McLeskey Jr., J.T., 2014. Comparison of genetic algorithm to particle swarm for constrained simulation-based optimization of a geothermal power plant, Advanced Engineering Informatics, 28, pp. 81-90.

Eghbal, M., Kumar Saha, T., Hasan, K.N., 2011. Transmission Expansion Planning by Metaheuristic Techniques: A comparison of Shuffled Frog Leaping Algorithm, PSO and GA, Power and Energy Society General Meeting, 2011 IEEE, USA, 12303073.

Elbeltagia, E., Hegazyb, T., Grierson, D., 2005. Comparison among five evolutionary-based optimization algorithms, Advanced Engineering Informatics, 19, pp. 43–53.

Finn, A., 2013. Nitrogen removal, Costain energy and process, LNGINDUSTRY.

Fu C., Gundersen, T., 2012. Using exergy analysis to reduce power consumption in air separation units for oxy-combustion processes, Energy, 44, pp. 60-68.

GPSA Engineering Data Book, Gas Processors Suppliers Association, 2004. Hydrocarbon Recovery: Nitrogen Rejection Unit, Tulsa, OK.

Hassan, R., Cohanim, B., Weck, O., 2005. A comparison of particle swarm optimization and the genetic algorithm, American Institute of Aeronautics and Astronautics, 46th AIAA/ASME/ASCE/AHS/ASC Structures, Structural Dynamics and Materials Conference, USA, AIAA2005-1897.

Healy, M.J., Finn, A.J., Halford, L., 1999. UK nitrogen-removal plant starts up, Oil & Gas Journal, 97 (5), pp. 36-41.

Hinderink, A.P., Kerkhof, F.P.J.M., Lie, A.B.K., De Swaan Arons, J., Van Der Kooi, H.J., 1996. Exergy analysis with a flowsheeting simulator - I. Theory; calculating exergies of material streams, Chemical Engineering Science, 51(20), pp. 4693-4700.

Höök, M., 2009. Depletion and Decline Curve Analysis in Crude Oil Production, Licentiate thesis, Global Energy Systems Department of Physics and Astronomy, Uppsala University.

Kennedy, J., Eberhart, R., 1995. Particle Swarm Optimization, Proceedings of IEEE International Conference on Neural Networks, 4, pp. 1942-1948.

Kerry, F.G., 2007. Industrial gas handbook: gas separation and purification, Boca Raton-Florida, USA: CRC Press.

Khan, M.S., Lee, M., 2013. Design optimization of single mixed refrigerant natural gas liquefaction process using the particle swarm paradigm with nonlinear constraints, Energy, 49, pp. 146-155

Kotas T.J., 1995. The exergy method of thermal plant analysis. 2nd ed. MalabarFlorida,USA: Krieger Publishing Company.

Krooss, B.M., Littke, R., Muller, B., Frielingsdorf, J., Schwochau, K., Idiz, E.F., 1995. Generation of nitrogen and methane from sedimentary organic matter: implications on the dynamics of natural gas accumulations, Chemical Geology, 126, pp. 291-318.

Kuo, J.C., Wang, K.H., Chen, C., 2012. Pros and cons of different Nitrogen Removal Unit (NRU) technology, Journal of natural gas science and engineering, 7, pp. 52-59.

MacKenzie, D., Cheta, I., Burns, D., 2002. Nitrogen removing, Hydrocarbon Engineering.

McCabe, W.L., Thiele, E.W., 1925. Graphical design of fractionating columns, Industrial and Engineering Chemistry, 17 (6), pp. 605–611.

Panduro, M.A., Brizuela, C.A., 2009. A comparison of genetic algorithms, particle swarm optimization and the differential evolution method for the design of scannable circular antenna arrays. Progress in Electromagnetics Research 13(2), pp. 171–186.

Rezakazemi, M., Dashti, A., Asghari, M., Shirazian, S., 2017. H2-selective mixed matrix membranes modeling using ANFIS, PSO-ANFIS, GA-ANFIS, International Journal of Hydrogen Energy, 42, pp. 15211-15225.

Rufford, T.E., Smart, S., Watson, G.C.Y., Graham, B.F., Boxall, J., Dinizda Costa, J.C., Maya, E.F., 2012. The removal of CO2 and N2 from natural gas: A review of conventional and emerging process technologies, Journal of petroleum science and engineering, 94, pp. 123-154.

Sadeghzadeh, H., Ehyaei, M.A., Rosen, M.A., 2015. Techno-economic optimization of a shell and tube heat exchanger by genetic and particle swarm algorithms, Energy Conversion and Management, 93, pp. 84-91.

Siddhartha, Sharma N, Varun, 2012. A particle swarm optimization algorithm for optimization of thermal performance of a smooth flat solar air heater, Energy, 38, pp. 406-413

Soares Pinto, F., Zemp, R., Jobson, M., Smith, R., 2011. Thermodynamic optimisation of distillation columns, Chemical Engineering Science, 66, pp. 2920-2934.

Timmerhaus, K.D., Flynn, T.M., 1989. Cryogenic Process Engineering, Springer US, pp. 287-376.